

N_2 complex **2**, the butylsilyl derivative **5**, having the formula $\{[P_2N_2]Zr\}_2(\mu-\eta^2-N_2SiH_2Bu^t)(\mu-H)$, was isolated as yellow needles (Fig. 1). In the 1H NMR spectrum, there were observed two broad singlets at 5.07 and 4.80 ppm due to two inequivalent Si-H protons. There was also a broad quintet at 1.53 ppm that collapsed to a broad singlet upon ^{31}P decoupling; this resonance can be assigned to a $Zr_2(\mu-H)$ moiety on the basis of its similarity to the signal observed at 2.07 ppm for **3**, which was proposed to be a bridging hydride. This assignment suggests that, analogous to **3**, heterolytic cleavage of the Si-H bond has occurred, with the silyl fragment now bound to the N_2 unit. The solution characteristics of **5** are very similar to those observed for **3**, supporting the proposed solution structure for **3**. The proposition that both **3** and **5** contain a hydride bridging the two Zr centers is reinforced by the low-temperature, solid-state structure of **5** (**11**) (Fig. 4), in which the Bu^tSiH_2 fragment is bonded to the bridging N_2 unit, with the remaining silyl-derived H atom symmetrically bridging the two Zr atoms; the bridging hydride was located from the difference Fourier maps and isotropically refined and is at a similar Zr-H bond distance to those observed for the $\mu-\eta^2-H_2$ unit in **4**. The incorporation of the silyl group at N-1 has resulted in a lengthening of the N-N bond distance from 1.43(1) Å in **2** to 1.530(4) Å in **5**.

The fact that coordinated N_2 can be induced to react stoichiometrically with H_2 and silanes suggests that other transformations of the N_2 moiety are possible using complexes with the appropriate combination of ancillary ligands and central metal. Further studies are needed to determine if the reactions reported here can be incorporated into catalytic cycles.

REFERENCES AND NOTES

- S. Gambarotta, *J. Organomet. Chem.* **500**, 117 (1995).
- G. Ertl, in *Catalytic Ammonia Synthesis*, J. R. Jennings, Eds. (Plenum, New York, 1991).
- M. K. Chan *et al.*, *Science* **260**, 792 (1993).
- G. J. Leigh, *ibid.* **268**, 827 (1995); C. E. LaPlaza and C. C. Cummins, *ibid.*, p. 861; M. Hidai and Y. Mizobe, *Chem. Rev.* **95**, 1115 (1995); G. J. Leigh, *J. Mol. Catal.* **47**, 363 (1988); R. A. Henderson, *Transition Met. Chem.* **15**, 330 (1990); ———, G. J. Leigh, C. J. Pickett, *Adv. Inorg. Chem. Radiochem.* **27**, 197 (1983); J. Chatt, J. R. Dilworth, R. L. Richards, *Chem. Rev.* **78**, 589 (1978).
- G. J. Leigh, *Acc. Chem. Res.* **25**, 177 (1992); B. B. Kaul, R. K. Hayes, T. A. George, *J. Am. Chem. Soc.* **112**, 2002 (1990), and references therein.
- J. Chatt, G. A. Heath, G. J. Leigh, *Chem. Commun.* **1972**, 444 (1972); H. M. Colquhoun, *Acc. Chem. Res.* **17**, 23 (1984); Y. Ishii, M. Kawaguchi, Y. Ishino, T. Aoki, M. Hidai, *Organometallics* **13**, 5062 (1994); K. Komori, H. Oshita, Y. Mizobe, M. Hidai, *J. Am. Chem. Soc.* **111**, 1939 (1989); H. Seino, Y. Ishii, T. Sasagawa, M. Hidai, *ibid.* **117**, 12181 (1995).
- J. M. Manriquez, D. R. McAlister, R. D. Sanner, J. E. Bercaw, *J. Am. Chem. Soc.* **100**, 2716 (1978).
- M. Hidai, K. Tominari, Y. Uchida, *ibid.* **94**, 110 (1972); T. A. George and R. C. Tisdale, *Inorg. Chem.* **27**, 2909 (1988).
- M. D. Fryzuk, M. Mylvaganam, J. D. Cohen, T. M. Loehr, *J. Am. Chem. Soc.* **116**, 9529 (1994); M. D. Fryzuk, T. S. Haddad, M. Mylvaganam, D. H. McConville, S. J. Rettig, *ibid.* **115**, 2782 (1993).
- M. D. Fryzuk, J. B. Love, S. J. Rettig, *Chem. Commun.* **1996**, 2783 (1996).
- Crystal data for **2**: formula, $C_{48}H_{64}N_6P_4Si_8Zr_2$; molecular weight $M = 1276.25$; lattice system, orthorhombic; space group $Ccca(\#68)$; temperature = $21.0^\circ C$; lattice parameters $a = 14.290(3)$ Å, $b = 19.213$ Å, and $c = 24.033(2)$ Å; unit cell volume $V = 6598(1)$ Å³; calculated density $D_{calc} = 1.285$ g cm⁻³; number of molecules in the unit cell $Z = 4$; linear absorption coefficient $\mu = 52.63$ cm⁻¹; empirical absorption correction; CuK α rays with graphite monochromator recorded on a Siemens SMART platform CCD diffractometer; 3499 measured reflections; 1649 reflections used with $I > 3\sigma(I)$; maximum diffraction angle $2\theta = 155^\circ$; 155 varied parameters; non-H atoms were refined anisotropically, H atoms were fixed in calculated positions with C-H = 0.98 Å; full least square matrix refinement; reliability factor $R = 0.042$; weighted reliability factor $R_w = 0.041$. Crystal data for **3**: formula $C_{48}H_{66}N_6P_4Si_8Zr_2$; $M = 1278.27$; lattice system, orthorhombic; space group $P2_12_12_1$; temperature = $173(2)$ K; lattice parameters $a = 12.2256(1)$ Å, $b = 21.0139(2)$ Å, and $c = 24.7043(3)$ Å; $V = 6346.72(11)$ Å³; $D_{calc} = 1.338$ g cm⁻³; $Z = 4$; $\mu = 0.617$ mm⁻¹; MoK α rays with graphite monochromator recorded on a Siemens SMART platform CCD diffractometer; 32,406 measured reflections; 11,145 reflections used with $I > 2\sigma(I)$; $\Theta_{max} = 25.03^\circ$; 721 varied parameters; non-H atoms were refined anisotropically, H1 and H2 were refined positionally and isotropically, and all other H atoms were placed in ideal positions and refined as riding atoms; full least square matrix refinement; $R = 0.0336$; $R_w = 0.0634$. Crystal data for **5**: formula $C_{52}H_{66}N_6P_4Si_8Zr_2$; $M = 1364.48$; lattice system, monoclinic; space group $C2/c$; temperature = $173(2)$ K; lattice parameters $a = 49.1499(2)$ Å, $b = 13.0446(2)$ Å, and $c = 24.0133(1)$ Å, $\beta = 116.579(1)^\circ$; $V = 13768.8(2)$ Å³; $D_{calc} = 1.316$ g cm⁻³; $Z = 8$; $\mu = 0.589$ mm⁻¹; MoK α rays with graphite monochromator recorded on a Siemens SMART platform CCD diffractometer; 34,508 measured reflections; 12,143 reflections used with $I > 2\sigma(I)$; $\Theta_{max} = 25.10^\circ$; 794 varied parameters; non-H atoms were refined anisotropically, the butyl chain refined as a split atom model with an occupancy of 0.74(2) to 0.26(2), the bridging hydride H1A was refined positionally and isotropically, and all other H atoms were placed in ideal positions and refined as riding atoms; full least-square matrix refinement; $R = 0.0491$; $R_w = 0.1223$.
- L. E. Sutton, *Tables of Interatomic Distances and Configuration in Molecules and Ions* (Chemical Society Spec. Publ. 11, Chemical Society, London, 1958).
- M. R. Smith III, T.-Y. Cheng, G. L. Hillhouse, *J. Am. Chem. Soc.* **115**, 8638 (1993).
- G. J. Kubas, *Acc. Chem. Res.* **21**, 120 (1988).
- P. G. Jessop and R. H. Morris, *Coord. Chem. Rev.* **121**, 155 (1992).
- J. E. Gozum and G. S. Girolami, *J. Am. Chem. Soc.* **113**, 3829 (1991); J. E. Gozum, S. R. Wilson, G. S. Girolami, *ibid.* **114**, 9483 (1992).
- H. H. Brintzinger, *J. Organomet. Chem.* **171**, 337 (1979).
- J. P. Collman *et al.*, *J. Am. Chem. Soc.* **112**, 8206 (1990).
- Z. He, S. Nefedov, N. Lugan, D. Neibecker, R. Mathieu, *Organometallics* **12**, 3837 (1993); C. Hampton, W. R. Cullen, B. R. James, *J. Am. Chem. Soc.* **110**, 6918 (1988); T. Arliguie, B. Chaudret, R. H. Morris, A. Sella, *Inorg. Chem.* **27**, 598 (1988).
- X.-L. Luo *et al.*, *J. Am. Chem. Soc.* **116**, 10312 (1994); *ibid.* **117**, 1159 (1995); J. J. Schneider, *Angew. Chem. Int. Ed. Engl.* **35**, 1068 (1996).
- Funding for this research was generously provided by the Natural Sciences and Engineering Research Council of Canada.

20 November 1996; accepted 22 January 1997

Soft-Landing of Polyatomic Ions at Fluorinated Self-Assembled Monolayer Surfaces

S. A. Miller, H. Luo, S. J. Pachuta, R. G. Cooks*

A method of preparing modified surfaces, referred to as soft-landing, is described in which intact polyatomic ions are deposited from the gas phase into a monolayer fluorocarbon surface at room temperature. The ions are trapped in the fluorocarbon matrix for many hours. They are released, intact, upon sputtering at low or high energy or by thermal desorption, and their molecular compositions are confirmed by isotopic labeling and high-resolution mass measurements. The method is demonstrated for various silyl and pyridinium cations. Capture at the surface is favored when the ions bear bulky substituents that facilitate steric trapping in the matrix.

Modification of surfaces to control their chemical and physical properties is of interest in many areas of science, including microelectronics, catalysis, optics, and electrochemistry (1). High-energy ion beams ($>10^3$ eV) have long been used for thin-film modification, especially in the technique of ion implanta-

tion (2), and collisions of hyperthermal energy (<100 eV) gas-phase ions are beginning to be used for surface modification. For example, metal carbides can be generated by exposing metals such as nickel, tungsten, and gold to beams of C^+ ions (20 to 200 eV) (3); CO can be absorbed molecularly on nickel(111) when delivered as the molecular ion (4); and methyl groups can be chemisorbed to a platinum surface when gaseous methyl ions are used as reagents (5). Complex ion-surface reactions also occur in this energy regime; for example,

S. A. Miller, H. Luo, R. G. Cooks, Department of Chemistry, Purdue University, West Lafayette, IN 47907, USA. S. J. Pachuta, 3M Corporate Research Labs, 3M Center, St. Paul, MN 55144, USA.

*To whom correspondence should be addressed.

there is evidence for transhalogenation (6) between the projectile ion and a fluorinated self-assembled monolayer (F-SAM) (7) surface. When 60-eV SiCl_4^+ ions collide with an F-SAM surface, SiCl_2F^+ is scattered, and subsequent characterization of the modified surface by 60-eV Xe^+ chemical sputtering yields a signal at a mass/charge ratio (m/z) of 85, indicative of the CF_2Cl functional group at the interface.

We report a new process, surface modification by soft-landing, which involves intact deposition of polyatomic ions (8) using low-energy ion beams. These observations add to the already rich chemistry of hyperthermal ion-surface collisions, including reactive, charge transfer, and dissociative processes (9). All of these processes are characterized by the almost unlimited variety of chemical reagent species and the control over the interaction energy, dose, and isotopic composition offered by mass spectrometric methods.

To illustrate soft-landing, Fig. 1 shows the deposition of $(\text{CH}_3)_2\text{SiNCS}^+$ projectile ions into an F-SAM surface (10). Two $(\text{CH}_3)_2\text{SiNCS}^+$ ions have penetrated the surface to different depths, and a third is approaching the F-SAM surface (11). The bulky substituent groups are important in facilitating soft-landing by steric interactions (see be-

low). This is a simplified representation of the soft-landing process, and the surface disorder produced by ionic collisions is not shown.

Consider the sterically bulky and strongly bonded silyl ether ion, $(\text{CH}_3)_3\text{SiOSi}(\text{CH}_3)_2^+$ (m/z 147), generated by electron impact on hexamethyldisiloxane. This ion was mass-selected, decelerated to 10 eV, and allowed to collide with a monolayer surface of the thiol, $\text{CF}_3(\text{CF}_2)_7(\text{CH}_2)_2\text{SH}$, self-assembled on a polycrystalline gold substrate. The F-SAM surface (12) was examined before and after 1 hour of deposition of the ether ion (8×10^{-10} A per 50 mm^2) (13) with the use of 60-eV $^{132}\text{Xe}^+$ sputtering for surface analysis. The sputtered ion spectrum (Fig. 2) showed only a single new prominent ion, also with m/z 147, after the deposition experiment. After storage of the treated surface in laboratory air for 1 day, the m/z 147 signal had decreased by only 30%; the signal was still observable after 4 days. For various experiments, storage of the treated surfaces in vacuum extended the lifetime of the deposited ion for as long as 14 days.

The conclusion that a polyatomic ion can be deposited intact into a monolayer surface and then liberated by $^{132}\text{Xe}^+$ sputtering is supported by the experiments summarized in Table 1. These results suggest that successful soft-landing and retrieval of polyatomic ions is

favored by relatively bulky steric groups. Presumably, these structural features assist in trapping the ion in the F-SAM matrix as well as in reducing the rate of its removal through chemical reaction (the surrounding hydrophobic environment presumably acts to protect deposited ions from polar reagents such as water vapor).

In a typical experiment, the total ion dose required to saturate the surface with soft-landed ions, as measured by intermittent $^{132}\text{Xe}^+$ sputtering, was 1×10^{13} ions. If the unit cell for the F-SAM chains is assumed to be 5.8 \AA on a side (11), the total dose corresponds to $\sim 7\%$ of a monolayer, although the actual coverage will be reduced by a factor corresponding to the efficiency of soft-landing. When a surface was dosed at subsaturation levels with 4×10^{12} projectile ions and then sputtered for long enough to release all of the soft-landed ions, $\sim 2 \times 10^{10}$ ions were released (14). The ratio of these two numbers (0.5%) is a measure of the combined efficiency of the soft-landing and chemical sputtering processes; although the two factors are difficult to quantify separately, it is clear that most ion impact events do not result in successful ion trapping at the surface.

Independent confirmation of the nature of the soft-landed species was obtained by performing an experiment in which 10-eV

Fig. 1. Three-dimensional molecular modeling representation of the soft-landing process for $(\text{CH}_3)_2\text{SiNCS}^+$ projectile ions impinging on an F-SAM monolayer surface. Color code: orange, Au; yellow, S; gray, C; cyan, H; green, F; magenta, Si; and blue, N.

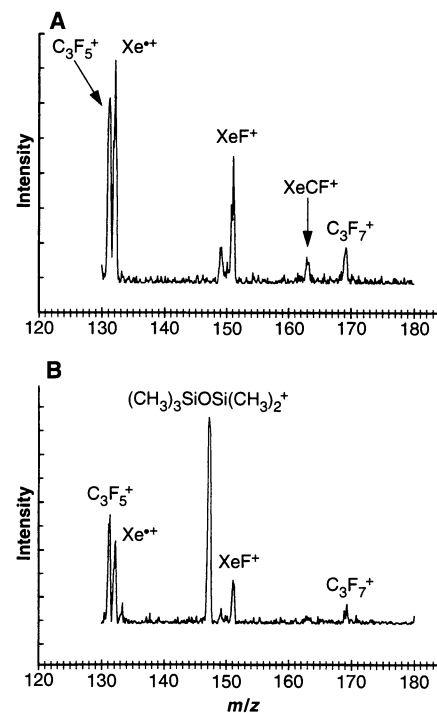
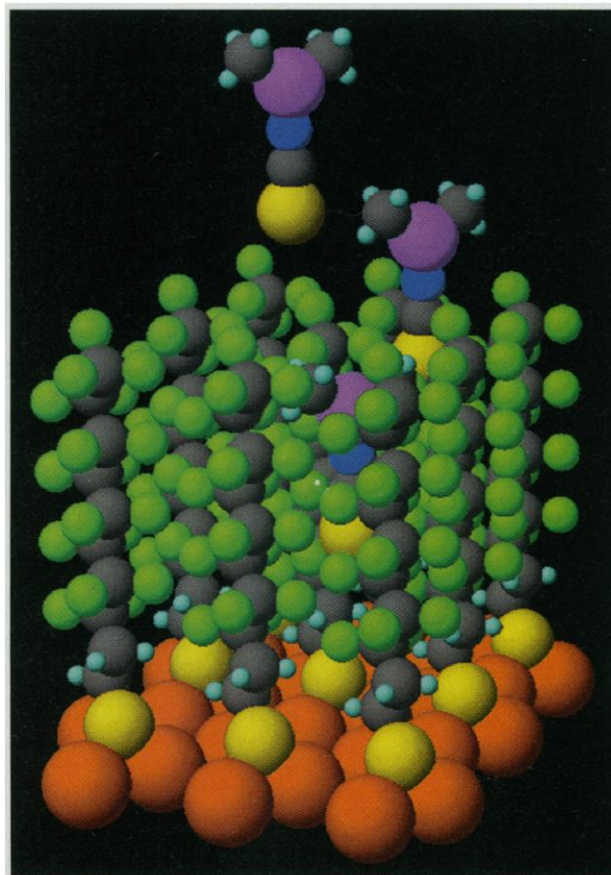


Fig. 2. Mass spectrum recorded by 60-eV $^{132}\text{Xe}^+$ sputtering of (A) an F-SAM surface and (B) the same surface after treatment for 1 hour at 5-eV collision energy with $(\text{CH}_3)_3\text{SiOSi}(\text{CH}_3)_2^+$ ions (m/z 147), at a total dose corresponding to $\sim 7\%$ of a monolayer.

beams of $^{35}\text{ClCH}_2(\text{CH}_3)_2\text{SiOSi}(\text{CH}_3)_2^+$ (m/z 181) and $^{37}\text{ClCH}_2(\text{CH}_3)_2\text{SiOSi}(\text{CH}_3)_2^+$ (m/z 183) were used in succession as projectiles while controlling the time of deposition so as to treat the F-SAM surface with approximately equal amounts of the ^{35}Cl and ^{37}Cl isotopes. These ions fragment upon collision at the surface to yield fragments, m/z 153 and m/z 155, that can be retained at the interface. [The ion $\text{ClCH}_2(\text{CH}_3)_2\text{SiOSi}(\text{CH}_3)_2^+$ (m/z 181 and 183, respectively, in the ^{35}Cl and ^{37}Cl isotopic forms) is known from its behavior in the gas phase to fragment readily by loss of C_2H_4 to give product ions of m/z 153 and 155.] Deposition of m/z 153 and m/z 155 ions was confirmed by 60-eV $^{132}\text{Xe}^{++}$ sputtering. The sample was then shipped to Minnesota for high-resolution time-of-flight secondary ion mass spectrometry (TOF-SIMS) analysis (15), which showed the expected exact masses [expected for $\text{C}_3\text{H}_{10}\text{Si}_2\text{O}^{35}\text{Cl}^+$, 152.9959 amu, found, 153.00 amu; expected for $\text{C}_3\text{H}_{10}\text{Si}_2\text{O}^{37}\text{Cl}^+$, 154.9929 amu, found, 154.99 amu] in the expected, but unnatural, 1:1 abundance ratio.

The deposited polyatomic ions are present at the surface, at least in part, as charged species, because the projectile ions are liberated intact by low-energy sputtering and there is no evidence for the presence of species other than simple transformation products of the soft-landed ions. Further evidence that the projectile ions are present as such in the matrix comes from studies in which sputtering was performed with ions other than $^{132}\text{Xe}^{++}$. The results, shown in Table 2 for the particular case of the ion at m/z 153 [generated from $\text{ClCH}_2(\text{CH}_3)_2\text{SiOSi}(\text{CH}_3)_2^+$], demonstrate that there is no correlation between the recombination

energy of the projectile and the sputtered ion yield, which would be expected (16) if neutral molecules (radicals) were present at the surface and were being re-ionized by charge exchange. Variation of the collision energy of the sputtering projectile ions revealed that the onset of chemical sputtering of the F-SAM surface coincided with the release of the soft-landed species and that the abundance ratio of the soft-landed species (3-trifluoromethylbenzoyl ion) to the chemically sputtered ions from the surface (for example, CF_3^+) was constant over the collision energy range of 20 to 70 eV. These results suggest that C–C bond cleavage in the F-SAM surface is necessary to remove tightly held soft-landed species that are trapped intact as ions.

More evidence that ions are trapped as such in the monolayer surface was obtained by their thermal desorption in a mass spectrometer, operated with the ion source filament turned off (17). The chloro-containing ion, $\text{C}_3\text{H}_{10}\text{OSi}_2^{35}\text{Cl}^+$ (m/z 153), was thermally desorbed and detected intact, while a second F-SAM surface, modified with $\text{C}_3\text{H}_{10}\text{OSi}_2^{37}\text{Cl}^+$ (m/z 155), also released the intact deposited ion at m/z 155. Desorption of the soft-landed ions occurred at temperatures ranging from 300° to 400°C. These results demonstrate that F-SAM surfaces can be selectively modified by soft-landing of polyatomic ions at collision energies of ~5 to 10 eV. At higher energies, especially >20 eV, surface-induced dissociation tends to preclude deposition of intact ions into the surface; even at 10 eV, projectiles that readily dissociate upon collision may fragment, but these fragment ions may nevertheless be trapped. The modified surfaces prepared by soft-landing re-

tain the deposited material for relatively long periods, in or out of vacuum.

The failure of the soft-landed ions to be removed rapidly by chemical reaction may result from the strongly hydrophobic F-SAM matrix, which helps exclude reagents such as water, and from the steric bulk of the projectile ion itself, which helps to screen the reactive charge site from attack by reagents. The projectile ions are probably bound both by electronic factors (ion induced-dipole forces) and by steric factors. The latter may include entrapment in the disordered F-SAM chains. It is likely that the deposited ions occupy a variety of surface sites, with some being more strongly held than others. The deposition efficiency has not been quantitatively characterized but is known to vary with the nature of the ion and the energy with which it is delivered to the surface.

Although comparisons can be made with other materials in which ions are trapped in a confined environment, in-

Table 2. Effect of the recombination energy of the sputtering ion on sputtered ion yields.

Sputtering ion	Recombination energy (eV)	Sputtered ion yield*
Ar $^{++}$	15.76	0.30
Kr $^{++}$	14.0	0.39
Xe $^{++}$	12.13	1
3-Chloropyridine molecular ion	9.58	0.37
Ferrocene molecular ion	6.75	0.27

*Expressed as the abundance of m/z 153 normalized to the abundance of the sputtering ion beam current. The calculated value was further normalized with respect to the result obtained with Xe^{++} sputtering.

Table 1. Summary of some soft-landing experiments.

Projectile ion and energy	Sputtered ions (m/z)*	Comments
$\text{C}_5\text{H}_{15}\text{OSi}_2^+$ (m/z 147), 5 to 10 eV	147, 73	Relative intensity decreased with time in and out of vacuum
$\text{C}_5\text{H}_{14}\text{OSi}_2^{35}\text{Cl}^+$ (m/z 181), 10 eV	153, 137, 73, 59, 79	m/z 153 present a few days after sample was removed from vacuum but with smaller intensity
$\text{C}_5\text{H}_{14}\text{OSi}_2^{37}\text{Cl}^+$ (m/z 183), 10 eV	155, 139, 73, 59, 81	m/z 155 present a few days after sample was removed from vacuum but with smaller intensity
$(\text{CH}_3)_2\text{SiNCS}^+$ (m/z 116), 10 to 20 eV	116	Relative intensity slowly decreased with time in vacuum (14 days)
SiNCS^+ (m/z 86), 10 eV	Not observed	
H_2SiNCS^+ (m/z 88), 10 eV	Not observed	
$\text{C}_3\text{H}_{10}\text{OSi}_2^{35}\text{Cl}^+$ (m/z 153), 5 to 10 eV	153, 137, 73, 59, 79	m/z 153 had a smaller relative intensity than in experiments using m/z 181 as the projectile
$\text{C}_3\text{H}_{10}\text{OSi}_2^{37}\text{Cl}^+$ (m/z 155), 5 to 10 eV	155, 139, 73, 59, 81	m/z 155 had a smaller relative intensity than in experiments using m/z 183 as the projectile
Pyridine molecular ion (m/z 79), 5 to 10 eV	Not observed	
3-Chloropyridine molecular ion (m/z 113), 5 to 10 eV	Not observed	
2,6-Dimethylpyridine molecular ion (m/z 107), 5 to 10 eV	107, 106, 108	
3,5-Dimethylpyridine molecular ion (m/z 107), 5 to 10 eV	107, 106, 108	
2,4,6-Trimethylpyridine molecular ion (m/z 121), 5 to 10 eV	122, 121, 120	Sputtered ions observable many hours after deposition but with low intensity (<1% relative abundance)
Protonated 2,4,6-trimethylpyridine ion (m/z 122), 5 to 10 eV	122, 123, 121	Intensities of m/z 121 and m/z 123 were only about one-fifth the intensity of m/z 122

*Sputtering by 60-eV Xe^{++} ; data exclude ions present in the blank. The sputtered ions are listed in order of decreasing abundance.

cluding ions trapped in C₆₀ (18) and ship-in-a-bottle synthesis of ions trapped in zeolites (19), the distinctive materials produced with our method are monolayer, room-temperature matrices that hold molecularly dispersed polyatomic cations. The implications for spectroscopy are apparent. The placement of isolated ions a few angstroms from a metal should give rise to interesting spectroscopic effects associated with the mixing of the discrete molecular orbitals of the matrix-isolated ions and the diffuse bands of the metal. The potential for preparing surfaces and interfaces with unusual electronic and magnetic properties is also evident. The extraordinary selectivity offered by the availability of a wide variety of projectile ions should allow the production of long-lived metastable structures of various types at self-assembled monolayer surfaces.

REFERENCES AND NOTES

1. A. Aviram, *Molecular Electronics: Science and Technology* (American Institute of Physics, New York, 1992); E. Kim, G. M. Whitesides, L. K. Lee, S. P. Smith, M. Prentiss, *Adv. Mater.* **8**, 139 (1996); K. K. Berggren *et al.*, *Science* **269**, 1255 (1995); D. Li *et al.*, *J. Am. Chem. Soc.* **112**, 7389 (1990); A. J. Bard *et al.*, *J. Phys. Chem.* **97**, 7147 (1993).
2. J. Shi *et al.*, *Nature* **377**, 707 (1995).
3. J. W. Rabalais and S. R. Kasi, *Science* **239**, 623 (1988).
4. H. Kang, S. R. Kasi, J. W. Rabalais, *J. Chem. Phys.* **88**, 5882 (1988).
5. D. Strongin and J. Mowlem, *Chem. Phys. Lett.* **187**, 281 (1991).
6. R. G. Cooks, T. Ast, T. Pradeep, V. H. Wysocki, *Acc. Chem. Res.* **27**, 316 (1994); T. Pradeep *et al.*, *J. Am. Soc. Mass Spectrom.* **6**, 187 (1995).
7. M. D. Porter, T. B. Bright, D. L. Allara, C. E. D. Chidsey, *J. Am. Chem. Soc.* **109**, 3559 (1987); F. Sun *et al.*, *ibid.* **118**, 1856 (1996).
8. For early attempts to perform this experiment, see V. Franchetti, B. H. Solka, W. E. Baitinger, J. W. Amy, R. G. Cooks, *Int. J. Mass Spectrom. Ion Phys.* **23**, 29 (1977).
9. R. G. Cooks, T. Ast, M. A. Mabud, *Int. J. Mass Spectrom. Ion Processes* **100**, 209 (1990); J. L. Jones, A. R. Dongre, A. Somogyi, V. H. Wysocki, *J. Am. Chem. Soc.* **116**, 8368 (1994); Q. Wu and L. Hanley, *ibid.* **115**, 1191 (1993); W. R. Koppers *et al.*, *Phys. Rev. B* **53**, 11207 (1996); M. J. Hayward *et al.*, *J. Am. Chem. Soc.* **118**, 8375 (1996).
10. The image in Fig. 1 was produced with the program CAChe, version 3.7 (CAChe Scientific, Beaverton, OR).
11. F-SAM chain spacings were set according to G. Liu *et al.*, *J. Chem. Phys.* **101**, 4301 (1994).
12. F-SAM surfaces were prepared by soaking the substrate in a 1 mM solution of CF₃(CF₂)₇(CH₂)₂SH in ethanol for at least a few days. The surfaces were then rinsed and sonicated in ethanol several times before modification by the low-energy ion beams. The substrate consists of a glass layer, 1.6 mm thick, covered with 50 Å of Ti and 1000 Å of polycrystalline gold.
13. Beam sizes were estimated using a highly focused 15-keV beam of Ga⁺ after modification of two F-SAM surfaces at 10 eV (area 50 mm²) and 60 eV (area 3 mm²).
14. The number of sputtered ions was estimated by converting the total analog-to-digital converter counts in the sputtered ion decay curve of the deposited species into an ion current and estimating corrections for the gain, transmission, and spot sizes of the experiment.

15. The high-resolution TOF-SIMS analysis was performed with a TFS series instrument (Charles Evans & Associates, Redwood City, CA) with 15-keV Ga⁺ ion sputtering. The TOF-SIMS data were taken about 36 hours after the surface sample was modified with C₃H₁₀Si₂O³⁵Cl⁺ (*m/z* 153) and C₃H₁₀Si₂O³⁷Cl⁺ (*m/z* 155) from projectile ions C₆H₁₄Si₂O³⁵Cl⁺ (*m/z* 181) and C₆H₁₄Si₂O³⁷Cl⁺ (*m/z* 183), respectively. The ions C₃H₁₀Si₂O³⁵Cl⁺ (*m/z* 153) and C₃H₁₀Si₂O³⁷Cl⁺ (*m/z* 155) had about equal intensities as determined by in situ 60-eV ¹³²Xe⁺ sputtering analysis before the sample was sent to 3M Center (St. Paul, MN) for TOF-SIMS analysis.
16. The cross section for sputtered ion yields is maximized when the recombination energy is in resonance with the ionization energy of the neutral molecule [see J. B. Hasted, *Physics of Atomic Collisions* (American Elsevier, New York, ed. 2, 1972), p. 612]. Neutralization and deposition of the resulting radicals into the surface is not precluded; this is likely to be one of the ion loss processes leading to low yields.
17. These experiments were performed with a Finnigan

TSQ 700 triple-quadrupole mass spectrometer with the ion source filament turned off. The sample was mounted on a specially constructed direct insertion probe that heated the surface from room temperature to 400°C in 40 s. Well-defined peaks from desorbed ions were observed in plots of ion abundance versus time. The trapped ions that are thermally released might not be as tightly held as those desorbed by ion impact.

18. R. Tellmann, N. Krawez, S.-H. Lin, I. V. Hertel, E. E. B. Campbell, *Nature* **382**, 407 (1996).
19. T. Tao and G. Maciel, *J. Am. Chem. Soc.* **117**, 12889 (1995).
20. Supported by NSF grant CHE-9223791. We thank B. Feng for assistance in the F-SAM surface preparation, D. Lantrip for the CAChe simulations, G. Chen for the triple-quadrupole data, Y. H. Yim for the trifluoromethylbenzoyl data, and T. Bein, W. N. Delgass, B. S. Freiser, H. W. Rohrs, and V. H. Wysocki for helpful comments.

15 October 1996; accepted 9 January 1997

Gliding Mechanism in the Late Permian Reptile *Coelurosauravus*

Eberhard Frey, Hans-Dieter Sues,* Wolfgang Munk

A complete skeleton of the oldest known flying reptile, *Coelurosauravus jaekeli*, from the Upper Permian of Germany, and reexamination of other specimens demonstrate that this animal had a gliding apparatus unlike that of any other tetrapod. The lateral gliding membrane was supported by radially disposed, greatly elongated bony rods of dermal origin in the thoracolumbar region, rather than by internal skeletal elements such as ribs and limb bones. The rods are independent of the ribcage and arranged in distinct bundles to form a cambered wing.

Extant and fossil terrestrial vertebrates have developed a diversity of gliding mechanisms (1, 2): (i) flattening of the body by drawing in the ventral surface of the body (the flying snake, *Chrysopelea*); (ii) spreading of webbed feet or membranous flaps along the hind edges of the limbs, in some instances accompanied by flattening of the body (some flying frogs such as *Hyla miliaria* and *Rhacophorus rheinwardtii*); (iii) expansion of a lateral skin fold between the fore- and hindlimbs [flying phalangers (Marsupialia), flying lemurs (Dermoptera), and flying squirrels]; (iv) expansion of a lateral membrane supported by elongated, flexible thoracolumbar ribs [as in the gliding lizard *Draco* (3)]; and (v), as (iv), but with elongated, rigid ribs, which form hinge-joints with the considerably enlarged transverse processes of the dorsal vertebrae [Late Triassic Kuehneosauridae (4, 5)]. Although many birds, especially large forms, are skilled gliders, bats rarely glide, perhaps

because they cannot control gliding and vary wing area as much as birds can (2). Here we describe a new skeleton of the oldest known flying tetrapod, *Coelurosauravus* (6, 7), and show that it had a different gliding mechanism from those examples mentioned above.

The Late Permian *Coelurosauravus* is a small diapsid reptile most closely related to the Neodiapsida, the clade including all archosaurian and lepidosaurian reptiles (8). The most diagnostic features of *Coelurosauravus* are the chameleon-like frill at the back of the skull roof, formed primarily by the squamosals, and the presence of numerous long, rodlike bones that supported a lateral gliding membrane (8, 9). These rods were originally misinterpreted as the fin rays of a coelacanth fish superimposed on a small reptilian skeleton and were, for the most part, removed during preparation of the holotype of *Coelurosauravus jaekeli* (10). When correctly recognized as genuine parts of the skeleton in other specimens, they were first interpreted as greatly elongated ribs (11) and later as the long distal segments of bipartite ribs (8). However, the supposed proximal rib elements (8) are short and strongly curved, much like the dorsal ribs in most other small reptiles. This feature is especially evident in an excellent-

E. Frey and W. Munk, Staatliches Museum für Naturkunde Karlsruhe, Erbprinzenstrasse 13, D-76133 Karlsruhe, Germany.
H.-D. Sues, Department of Palaeobiology, Royal Ontario Museum, 100 Queen's Park, Toronto, ON M5S 2C6, and Department of Zoology, University of Toronto, Toronto, ON M5S 3G5, Canada. E-mail: hdsues@rom.on.ca

* To whom correspondence should be addressed.